# Understanding the Li resource potential of granite hosted geothermal brines using near surface measurements

**Corresponding Author:**
Andrew David Robinson.

School of Natural and Environmental Sciences, Newcastle University, NE1 7RU, England.

Email: a.robinson11@ncl.ac.uk | andrew.d.robinson4@gmail.com

Telephone: +447713350378

https://orcid.org/0009-0009-1688-4158

**Authors:**

Sanem-Acikalin-Cartigny[1]

Gavin Stewart[1]

Brendan A. Bishop[2]

Leslie J. Robbins[2]

**Shannon L Flynn[1]**

[1]: School of Natural and Environmental Sciences, Newcastle University, NE1 7RU, England.
[2]: Department of Earth Sciences, University of Regina, 3737 Wascana Parkway, Regina, Saskatchewan S4S 0A2, Canada

**Funding Sources:**

*This paper contains work conducted during a PhD study undertaken as part of the Centre for Doctoral Training (CDT) in Geoscience and the Low Carbon Energy Transition and was funded by NeoEnergy Upstream whose support is gratefully acknowledged.*
*The interpretations and analyses were undertaken in the Drummond and Devonshire Buildings at Newcastle University, the underpinning financial and computer support for which is gratefully acknowledged. LJR and BAB would like to acknowledge funding from the Natural Sciences and Engineering Research Council of Canada (NSERC) in the form of a Canada Graduate Scholarship – Doctoral (BAB) and Discovery Grant (LJR: RGPIN-2021-02523)*

**Keywords:** Lithium, Geothermal, Energy transition, Principal Component Analysis, Mine water, Critical minerals.

This is a preprint submitted to EarthArxiv and is currently under review at Applied Geochemistry.

# Abstract

Unprecedented demand for lithium (Li) is being driven by its use in electric vehicle batteries. Currently, the majority of Li comes from pegmatite mining and salar brines, however, new sources such as geothermal brines will be required to meet future demand. The North Pennines, Northern England has been found to host brines with lithium concentrations exceeding 90 mg/L at depths of 411 to 996 m. However, deep subsurface water chemistry for the region is limited to a single abandoned borehole, necessitating the use of other techniques in assessing the resource potential of these brines. This work investigated the potential of surface and near-surface water samples from abandoned mine workings to expand the known geographic extent of the underlying Li brine resource. Li concentrations were 1.9 to 784 µg/L at the 44 locations sampled. Principal component, cluster, and covariate analyses identified two distinct water chemistry clusters mostly related to dimension 1 of the PCA (25.3% of variance): a brine related cluster which includes Alkalinity, Ca, Cd, Cl, F, K, Li, Mg, Na, Se, and $SO_4^{2-}$ ; a "near surface" or potentially orebody related group which includes Al, As, Cu, Eu, Fe, P, Pb, V, and Y. Two smaller clusters are present on the positive and negative axis of dimension two (15.4%); on the positive is B, Ba, Br, Cr, and pH, and on the negative, Co, Mn, Ni, Sc, Sr, and Zn. The Cambokeels Mine, 0.5 km from the original borehole had the highest Li concentration of 78.4 mg/L. However, the deep brine signature and Li enrichment was found at a cluster of mines 15 km away, significantly expanding the geographical extent of the North Pennine Li brine resource. These findings show that relatively low-cost elemental analysis and statistical analyses could be a promising exploration tool for regions with where there is limited data. Developing tools to readily identify potential Li resources in geothermal brines based on limited data will be essential for furthering the development of critical minerals in Britian.


# 1. Introduction

Lithium (Li) is experiencing unprecedented demand, with 80% driven by lithium-ion batteries for electric vehicles (Lindagato et al. 2023). Over the past five years (2019-2023) global Li production has increased from 98,300 to 197,000 Mt (USGS 2024, 2023, 2022, 2021). Lithium averages 0.18 ppm in seawater and 20 ppm in the continental crust, however, there are few environments where Li is naturally enriched to economic abundances (Kamienski et al. 2004). Consequently, greater than 98% of current Li production comes from two geologic settings; spodumene bearing pegmatites and salar evaporative brines in roughly equivalent amounts (Kavanagh et al. 2018).

Currently, spodumene deposits in Australia, China, and Brazil are the world's largest source of Li (Bowell et al. 2020). However, Li production from spodumene pegmatites requires energy-intensive hard rock mining, with a carbon footprint of 17.11 – 22.33 kg $CO_2$eq per kg of $Li_2CO_3$ produced (Mas-Fons et al. 2023). In contrast, Li production from salar brines have a carbon footprint that is 2.5-3 times lower (Kinch and Holman 2020). However, Li production from salars has an appreciable environmental footprint and high water demand. Salar deposits represent over half of the global Li reserve with the majority being in just three countries: Bolivia, Argentina, and Chile (Gruber et al. 2011). The formation of salar type deposits is rare due to the required co-occurrence of specific geological and climate conditions. The formation of Li salar brine depends on the lithology of the surrounding drainage basins (Munk et al. 2018). Li is thought to be sourced from later magmatic granites, ignimbrites, tuffs and/or volcanic ashes. Within the basin, the first evaporites form above the valley bottom and are sinks for major ions such as Na, Ca, Cl, and $SO_4$,

but leave Li in solution (Carmona et al. 2000; Vinante and Alonso 2006; Warren 2010). By the valley bottom, the brines are alkaline, sulphate, and calcium rich with Li concentrations of 1,000 – 5,000 mg/L (Munk et al. 2018) To summise. Li-rich brines share six common characteristics; arid climate; closed basin with a salar or salt lake; associated igenous and/or geothermal activity; tectonically driven subsidence; suitable lithium sources; sufficient time to concentrate brine (Munk *et al*. 2016). Production of Li from salar brines typically uses large pools utilizing solar concentration. While processing costs are lower than spodumene, it is weather dependent, space intensive, and the focus of environmental concerns such as air and water quality and permanent water loss in arid regions (Vera et al. 2023). With Li demand predicted to exceed supply by 2030 (Han et al. 2023), additional Li sources are being investigated (Miao et al. 2023).

Alternative, or unconventional, Li sources have gained attention as technological advances, driven by increased demand, have increased their viability. Unconventional Li deposits can be split into mineral deposits (e.g. volcanic sedimentary clays of Nevada USA, and Naomugeng, China (Li et al. 2021)), non-evaporitic brine deposits such as oilfield brines of North and South America (Ettehadi et al. 2024), and the geothermal waters of Italy, Germany, France, Czechia, Hungary, Turkey, and the UK (Dini et al. 2022; Sanjuan et al. 2022; Jancsek et al. 2023; Millot, Négrel, and Petelet-Giraud 2007; Karaca et al. 2013). Non-evaporitic brines have a much broader global distribution – and varied chemistry and Li sources – than their evaporitic counterparts. Geothermal and oilfield brines are becoming viable sources of Li due to technological advancements such as Direct Lithium Extraction (DLE). DLE bypasses evaporation by precipitating Li via the addition of solvents or through adsorption or ion-exchange (Stringfellow and Dobson 2021). A common strategy suggested to reduce risk and increase the returns on the high initial capital costs is the dual use of geothermal energy wells for Li extraction (Weinand et al. 2023). Heat would first be extracted for local heating, or direct energy production, with Li extracted before reinjection to recharge the geothermal reservoir (Goldberg et al. 2023; O'Sullivan et al. 2024). Oilfield brines often have high total dissolved solids (TDS) (>100,000 mg/L), where Li concentrations can exceed 80 mg/L (Ettehadi et al. 2024). Even in oilfield brines with high Li, the low Li to TDS ratio can negatively impact the efficacy of DLE, as well as issues with Mg, $H_2S$ and organics, despite this, oilfield brines are still seen as "low cost" due to the well infrastructure being in place.

Non-oilfield brines are also growing in commercial and academic interest, particularly in Europe due to a lack of conventional Li resources (Table 1). Broadly, geothermal brines enriched in Li are most commonly associated with intrusive felsic igneous bodies, such as granites and granitic pegmatites, which host primary Li minerals such as biotite micas like zinnwaldite and lepidolite, or in spodumene which does not occur in sufficient quantities or near enough to the surface to be mined directly. Even in igneous bodies without an identified primary Li mineral, such as the Upper Rhine Graben (URG), mica dissolution is still thought to represent the primary Li source for the brine hosted in the overlaying sandstone (Sanjuan et al. 2016).

The chemical characteristics of geothermal brines differ with the geological setting, though there are characteristics which are broadly shared among enriched Li brines: high alkali metal concentrations, particularly Na and K (>18 g/L), significant Cl (>25 g/L), and TDS exceeding tens of thousands of mg/L (Sanjuan et al. 2022) (Table 1). For example, Cesano is enriched in Na, K, Cl, $SO_4^{2-}$, Rb, and Cs, whereas the URG is similarly enriched in Na, K, Rb, but depleted in $SO_4^{2-}$. The TDS of geothermal brines is substantially lower compared to oilfield brines, which is favourable for the extraction of Li from these sources using DLE technologies.

**Table 1** Examples of Li concentration and host lithologies for Li enriched geothermal waters.

| Location | Li (mg/L) (Source) | Source of Li |
|---|---|---|
| URG (France & Germany) | 159-210 (Sanjuan et al. 2016) | Mica dissolution in micaceous sandstone |
| Cesano (Italy) | 380 (Dini et al. 2022) | Plio-quaternary magmatic rocks (Specific mineral and process unknown) |
| Battonya (Hungary) | 36 (Jancsek et al. 2023) | Chloritization of biotite micas |
| Cornwall (United Kingdom) | 220 (Boschetti 2022) | Mica dissolution in granite |
| North Pennines (United Kingdom) | 90 (Manning et al. 2007) | Suspected to be granite (Specific mineral and process unknown) |
| Tibetan Plateau (South-east Asia) | 7.98-239 (Li et al. 2022; WANG et al. 2021) | Degassing of semi-molten magma |
| Aigueperse (France) | 2.8-7.07 (Millot, Négrel, and Petelet-Giraud 2007) | Granite and volcanic (Specific mineral unknown) |
| Ngawha (New Zealand) | 9.7-12.3 (Mroczek, Climo, and Evans 2015) | Unknown – though hydrothermal biotites present |
| Dieng (Indonesia) | 77.31-99.4 (Suprapto and Yuliatin 2020) | Quaternary magmatic rocks (Specific mineral and process unknown) |
| Ayvacık Tuzla (Turkey) | 34.13-38.0 (Karaca et al. 2013) | Unknown |

While many geothermal Li brines are hosted in granitic systems, the Li source and ultimately concentration will vary depending on both the primary Li mineral and host mineralogy, as well as the weathering pathways and fluid geochemistry. In the North Pennines, England, the current knowledge of the Li brine resources is limited to a single borehole that had Li concentrations exceeding 90 mg/L within the underlying granitic batholith between 405-996 m depths (Manning et al. 2007). Understanding of the weathering processes and source minerals in this granite is limited, and there is very little subsurface data, which makes assessing this potential Li resource difficult and costly. Previous work on establishing background methane levels in groundwater has shown that subsurface mixing of deeper (<1km) fluids with surface and near-surface waters occurs in the near-surface. The vertical migration and mixing of these deeper high TDS waters resulted in detectable changes to surface and near-surface waters (Harkness et al. 2017; Eymold et al. 2018). This suggests that near-surface measurements may improve the understanding of the geographical extent, source, and pathways of the Li resource, in regions with limited subsurface data. In this study we test the potential of near-surface water analysis to detect faint signals of upwelling deeper Li-bearing brines, potentially moving along permeable pathways such as structural geologic features like faults. This is a key first-step in using readily available analyses to generate knowledge of the Li resource potential of at depth geothermal fluids in Northern England. Low cost knowledge generation for previously unassessed resources will be critical in identifying sufficient critical mineral sources to fuel the energy transition.

## 1.1 Geological setting

The North Pennines form the northern part of the larger Carboniferous Pennine Block Band basin Province. The structure encompasses 1500 $km^2$ that is bounded by the Ninety-fathom and Stublick faults (Tyne Valley) to the north, Stainmore Trough to the south, and Pennine Fault to the west. The block is composed of Carboniferous aged cyclothems made up by the limestone-hosted “coal measures”, the Stainmore and Alston formations, the great scar limestone group and an underlying series of basal beds which lie uncomformably over the early Devonian Aged batholith known as the Weardale Granite. The Carboniferous series is host to intrusive igneous sills and dykes and is cut north-south by the Burtreeford Disturbance, a compressional monocline which interrupts the regional fault system (Dunham 1990).

The region has extensive hydrothermal metalliferous mineralization primarily composed of ankerite, dolomite, siderite, quartz, fluorite, galena, and sphalerite that was deposited as veins and metasomatic flats. Mineralization is thought to have been emplaced by upwelling hydrothermal fluids related to the Weardale Granite (Bott and Smith 2018). The orebody has an extensive mining history, with hundreds of mine workings intercepting the veins and flats of the orebody (Colman, Ford, and Laffoley 1989).

The Carboniferous limestone formations and the associated intrusions and mineralisation are well understood due to mine works, however, the underlying Weardale granite is relatively understudied. The granite body has only twice been sampled from boreholes: first in 1961 at a depth of 390 m in Rookhope, and in 2004 outside Eastgate at a depth of 270 m. The Rookhope borehole is located at the approximate centre of the Weardale Pluton of the granite batholith, and was drilled with the intention of proving the existence of the granite body following gravity surveys (Dunham et al. 1961). Whereas, the Eastgate borehole targeted a fault, called the Slitt Vein, along which warm salty water with Li concentrations of 40-70 mg/L was found on the 100 m level of the Cambokeels Fluorite Mine (Manning and Strutt 1990). The fault cuts the Carboniferous strata and intersects the underlying granite (Manning et al. 2007). Before encountering the granite, both boreholes encountered a sticky white clay weathered top that was presumably kaolinitic. This was interpreted as indicating that the granite was subaerially exposed and therefore must predate the overlying sedimentary strata as well as the source of the metalliferous mineralising fluid (Dunham et al. 1961; Manning et al. 2007). During the drilling of the Eastgate borehole, Li concentrations of 7-50 mg/L were observed in the upper 335 m and increased to greater than 90 mg/L from 411-995 m (Manning et al. 2007). To date, Li rich water in the Cambokeel mine and Eastgate bore hole are the only Li-enriched fluids identified regionally, and all that is known of the potential subsurface Li resources of the North Pennines.

Currently, the granite is considered the most likely source of Li as the observed concentration was the highest and exceeded 80 mg/L at depth within the granite. However, there has yet to be mineralogical or elemental evidence establishing the presence or abundance of Li in the granite. The paucity of subsurface chemical data outside the Eastgate borehole makes estimating the Li resource potential in the North Pennines challenging, including determining the regional extent, or approximate volume of the Li brine reservoir. To address this, we use targeted near-surface water analyses to assess the potential for Li-bearing brines to migrate along faults or other permeable pathways.

# 2. Materials & Methodology

## 2.1 Sampling strategy

Between 2019 and 2022, 48 mine outflows were sampled across the North Pennines for a total of 78 samples which included repeat visits. Sampling focussed on mine workings with outflows where safe access was feasible, and landowner permission could be obtained. Ten mines were further sampled in the subsurface, with locations selected based on safety and accessibility.

## 2.2 Field and laboratory measurements

Conductivity, pH, oxidation-reduction potential (ORP), and temperature were measured in-situ using a Myron L Ultrameter II. Alkalinity was determined with a Hach AL-DT Field Alkalinity Kit, using an auto-titrator with a 1.6 M $H_2SO_4$ cartridge and bromocresol green.

Two samples were collected at each mine outflow and filtered through a 0.2 µm nylon membrane. Samples for cation analysis were acidified with 6 µl of 70% nitric acid per 10 ml. Cuttings from the Eastgate Borehole were digested in aqua regia using a CEM MARS 6 Microwave Digestion System and diluted 1:50 before analysis.

Prior to November 2023, major cations were measured by a Varian Vista MPX ICP-OES with simultaneous CCD using a Meinhard Nebulizer and cyclonic spray chamber. Later samples were measured on an Agilent 5800 with Meinhard Nebulizer and cyclonic spray chamber. Trace elements were measured via an Agilent 7700x ICP-MS with a Micromist Nebulizer and a cooled double concentric spray chamber, using He as the collision gas reaction cell. Composite standards for major cations were prepared to cover a range of 0.1 to 150 ppm, and for trace elements covering 0.0001 to 30 ppm. The analytical detection limit for Li in our primary samples was 5 µg/L.

Anions were measured via ion chromatography (IC) using a Dionex ICS-1000 with an AS40 autosampler, using an Ionpac AS14A, 4x250mm analytical column, 25 µL injection loop, and a pump rate of 1 ml/min. The eluent was a solution of 8.0 mM $Na_2CO_3$ and 1.0 mM $NaHCO_3$.

## 2.3 Statistical analysis

Statistical analysis and modelling were conducted using version 2023.03.386 of R Studio and the R language (R Core Team, 2023) (Posit Team, 2023). Principal component analysis (PCA) utilised the prcomp package (Becker *et al.* 1988) and plots were generated using the packages ggplot2 (Wickham, 2016), ggbiplot (Vu VQ, 2011), ggfortify (Tang *et al.* 2016), and factoextra (Kassambara *et al.* 2020).As geochemical data is compositional in nature, it is considered to be constrained; the variables cannot vary independently as they represent a sum to 100%, which forces covariance in the data to be negative, which biases results to the negative. Relative magnitude and variation of components is important for statistical analysis of compositional data, not the absolute values. A more robust explanation of the need for transformation is section 2.2 of (Bishop and Robbins 2024). As such, the centered log ratio (CLR) transformation was applied to the data before PCA using the composition package (van den Boogaart and Tolosana-Delgado 2008).

Regression modelling was conducted using rpart (Therneau *et al.* 2022) to produce a cluster analysis classification tree which had Li as the outcome variable using the ANOVA method of

analysis. Pearson correlation coefficients were calculated and plotted using corrplot (Friendly *et al.* 2002).

Rare earth elements were strongly co-correlated in model outputs (likely due to their similar chemistry) with seventeen near-identical variables resulting in unfeasibly high percentage of the variation explained. To avoid model overfitting, these rare earths were represented by Eu, Sc, and Y, as these had the greatest analytical accuracy.

Average values were not always representative because of outliers below feasible detection limits. Values below the detection limit were replaced with 0.5 x the detection limit (Dray and Josse 2015). We used the same approach to derive complete cases where data was unavailable. Analytes which had more replaced than measured values were removed from the analysis (e.g., $NO_3^-$, Mo). Further reduction of the number of analytes may have produced a model which accounted for a higher percentage of the variance within the samples, but the risk of overfitting the model through biased selection of variables discouraged this.

## 2.4 Two endmember mixing calculation

The deepest sample from the Eastgate borehole (Manning et al. 2007) was used as the end member representing "deep brine" chemistry, and the "near-surface" endmember was the mine water sample which most closely matched reference rainwater (Wilkinson et al. 1997), "high Capelcleugh adit". Both were used in a two-endmember mixing model using Cl as the conservative element where:

Eq.1 $$f_{BH} + f_{NS} = 1 = mine\ water\ sample$$

In which $f_{BH}$ was the contribution from deep brine and $f_{NS}$ was the contribution from near surface water. Using Cl as the conservative parameter the solute mass-balance equation is:

Eq.2 $$Cl_s = f_{BH} \cdot Cl_{BH} + f_{NS} \cdot Cl_{NS}$$

Where $Cl_s$ is the Cl concentration of the mine water sample and $Cl_{BH}$ and $Cl_{NS}$ are the Cl concentration of the borehole and near-surface end members, respectively. By rearranging equation 2, the fraction of borehole water in any mine water sample can be calculated as:

Eq.3 $$f_{BH} = \frac{Cl_s - f_{NS} \cdot Cl_{NS}}{Cl_{BH}}$$

## 2.5 Distribution mapping

Maps were produced using the open-source mapping software QGIS version 3.25.2 (QGIS, 2023), with geology maps from the British Geological Survey, and geology and Ordnance Survey maps obtained from Edina Digimap.

Subsurface maps were inaccessible for most mines sampled at depth, and the coordinates assigned relate with the mine outflows of these mines. The spatial uncertainty introduced by this is less than 200 m for most of the subsurface samples. Sites with more than one sampling instance had those numbers averaged before calculating the average for the field so that each mine had the same weighting.

# 3. Results

## 3.1 Lithium concentration of the Weardale Granite and hosted brine

In contrast to the relatively stable aqueous Li concentration in the granite of the Eastgate borehole below depths of 400 m ($\sim 90\ \mathrm{mg/L}$), Li concentration of the granite varied from 14 to 97.9 mg/kg (Figure 1). The “weathered top” of the granite, a kaolinitic soil regolith encountered around 280 m, had higher Li than the preceding sedimentary strata and subsequent samples at 34.1 mg/kg (280 m) compared to 26.8 mg/kg (275 m) and 14 mg/kg (300 m), respectively. The deepest sample (995 m) had the highest Li concentration, 99.2 mg/kg, and was one of the two depths (920 m) where the Li in the rock exceeded the concentration in solution.

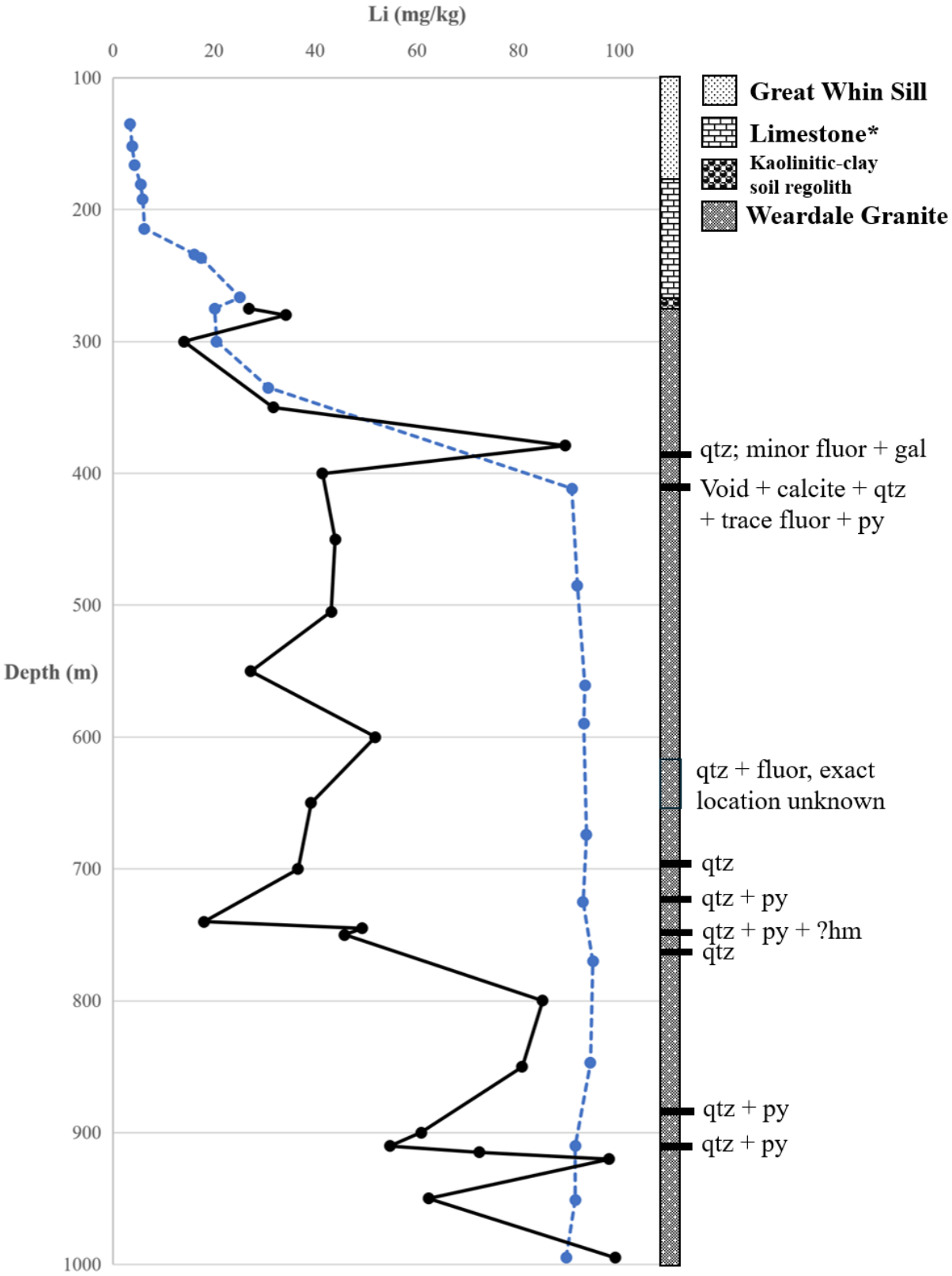


**Figure 1** Lithium concentration in the borehole cuttings (solid line) and water samples (dashed line) from the Eastgate Borehole. Water chemistry and simplified lithological log from Manning et al. 2007. Cutting inventroy has an accuracy of +/- 5m. Weathered top of the granite reached at 271 m, open fracture at 410 m. qtz, quartz; fluor, fluorite; gal, galena; py, pyrite; hm, hematite.

*Limestone; layered limestone, sandstone and mudstone cyclothems above the Weardale Granite, through which the Whin Sill and Dyke complex intrudes.

## 3.2 North Pennines surface and near-surface water chemistry

The mine outflows of the North Pennines had an average Li concentration of 24.2 µg/L (*Figure 2*), lower than the average concentration of seawater (Angino and Billings 1966). Before this study, the Cambokeels mine and the Eastgate borehole were the only reported Li concentrations due to the 100 µg/L detection limit for the Environment Agency's data. With a lower Li detection limit (5 µg/L) an additional two mine outflows were identified with Li concentrations exceeding the regional average, Scraithole Mine in the West Allen Valley (83 µg/L) and the Hagg's Level at Nenthead (49 µg/L) (Figure 2). The Li concentration at Scraithole Mine water was found to increase within the mine and was 138 µg/L, 600 m into the mine. The difference is indicative of a high-level dilution from meteoric water near to the mine portal and may impact other mine outflows.

Samples from Cambokeels mine had Li concentrations >150 µg/L, with concentrations ranging from 154 µg/L to 784 µg/L, varying with time of year and precipitation. Cambokeels is uniquely enriched, but it was the only mine over the central Weardale Pluton of the underlying granite with Li concentrations exceeding the average for the area. Additionally, Cambokeels is the only mine east of the Burtreeford disturbance to exceed the average. All other instances of elevated Li (greater than the average of 24.2 µg/L) are relatively localised to the northwest of the North Pennines and appear to not be directly related to any of the plutons of the Weardale Granite.

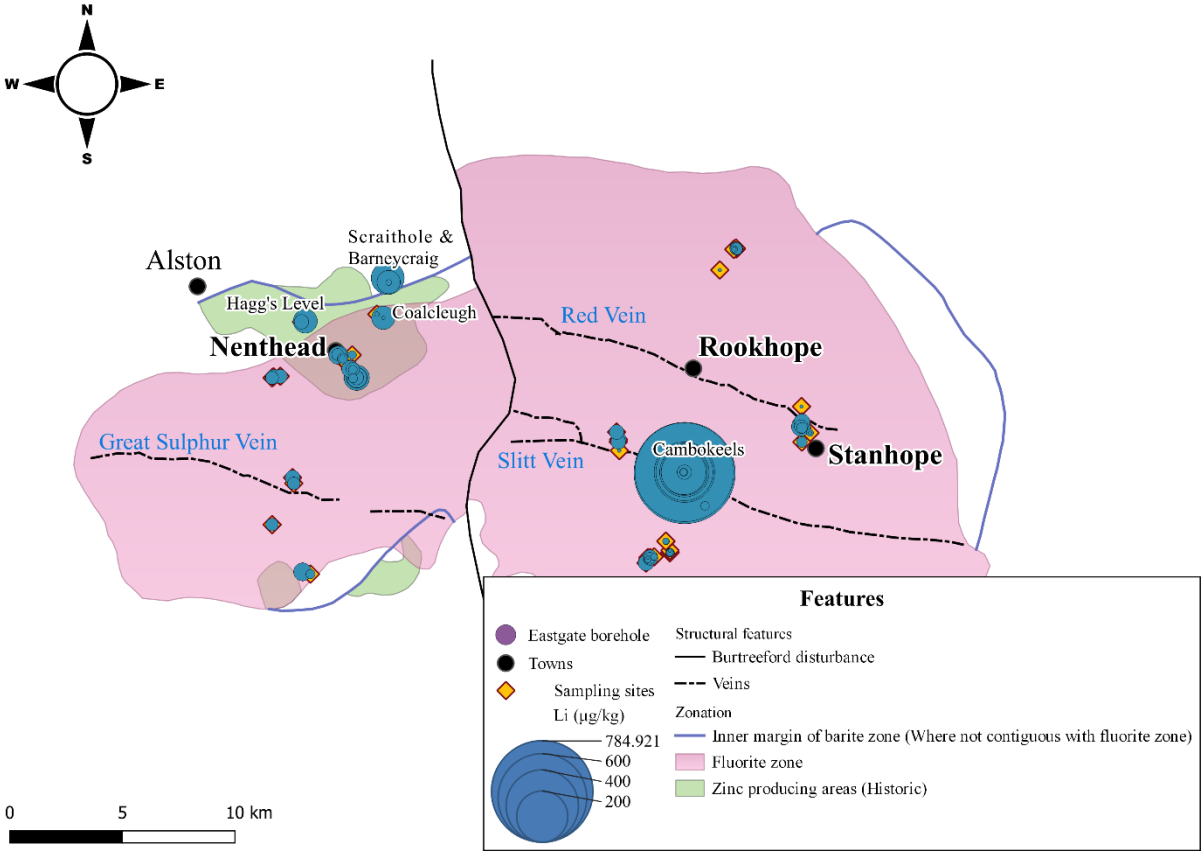

**Figure 2** Simplified map of the North Pennines showing the mineralisation zones and major fault features adapted from Dunham 1990. Sampling sites are show with circles proportional to the measured Li concentration and villages and mine adits with Li greater than the regional average are labelled.

## 3.3 Statistical analysis

Principal component analysis (PCA) of the sampled mine waters identified an elemental grouping with a positive correlation with Li: Alkalinity, Ca, Cd, Cl, conductivity F, K, Mg, Na, Se, and $SO_4^{2-}$ (*Figure 3*). A second grouping of Al, As, Cu, Eu, Fe, P, Pb, V, and Y. While these two groups were largely dominant in dimension 1 – with the second being slightly more relevant in dimension 2 than the first, two smaller, unrelated groups are present on the positive and negative axis of dimension two; on the positive is B, Ba, Br, Cr, and pH, and on the negative, Co, Mn, Ni, Sc, Sr, and Zn. Contributions of individual elements to PC1 and PC2 are shown in more detail in Appendix 1. Despite the large number of variables (36) and small sample size (78), 40.7% of variance was explained by PC1 and PC2 (*Figure 4*).

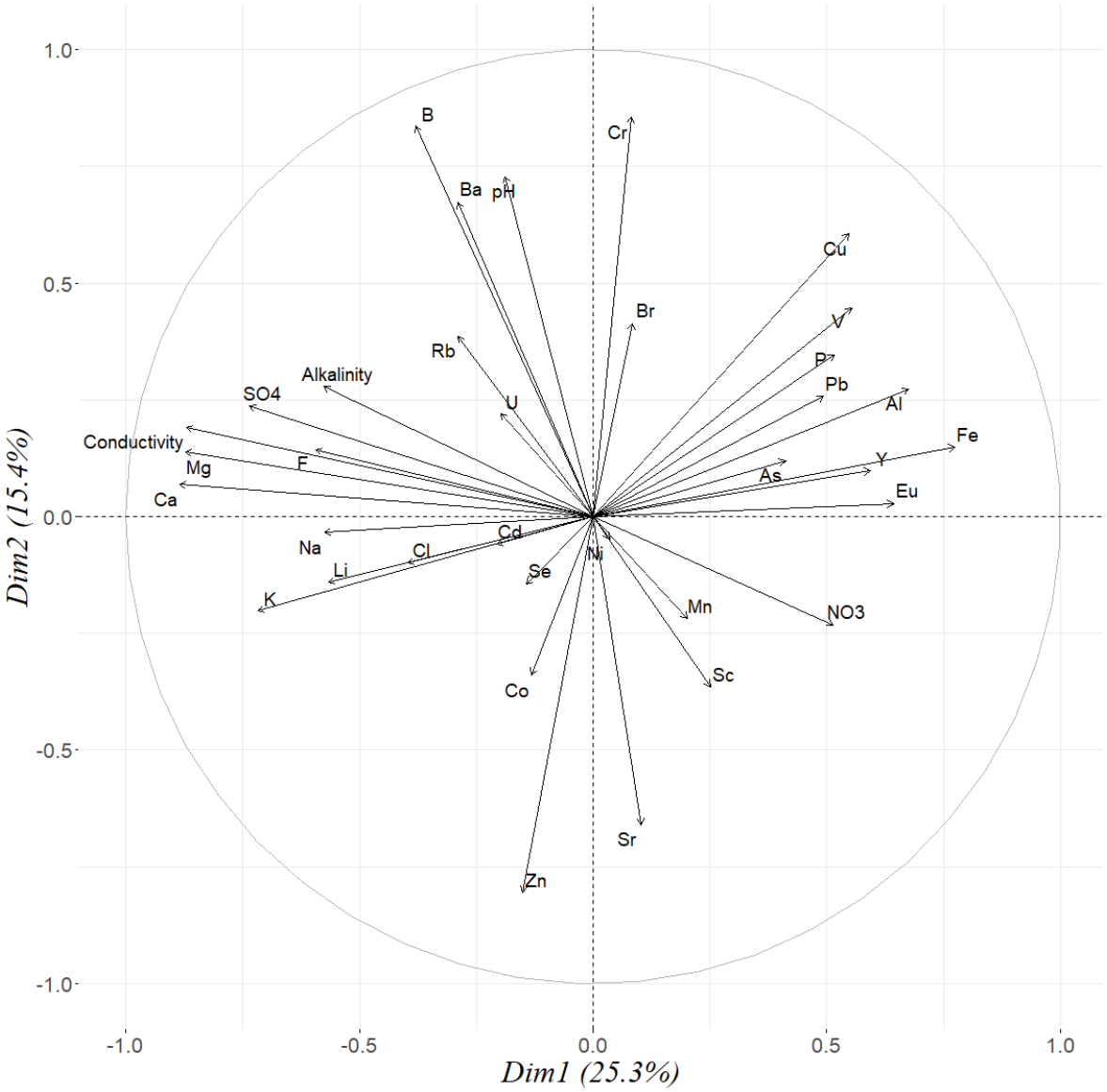


**Figure 3** Loading plot of variables contribution to Principal Component 1 (25.3%) and Principal Component 2 (15.4%) from a principal component analysis of mine water samples. N=78, Variables = 35.

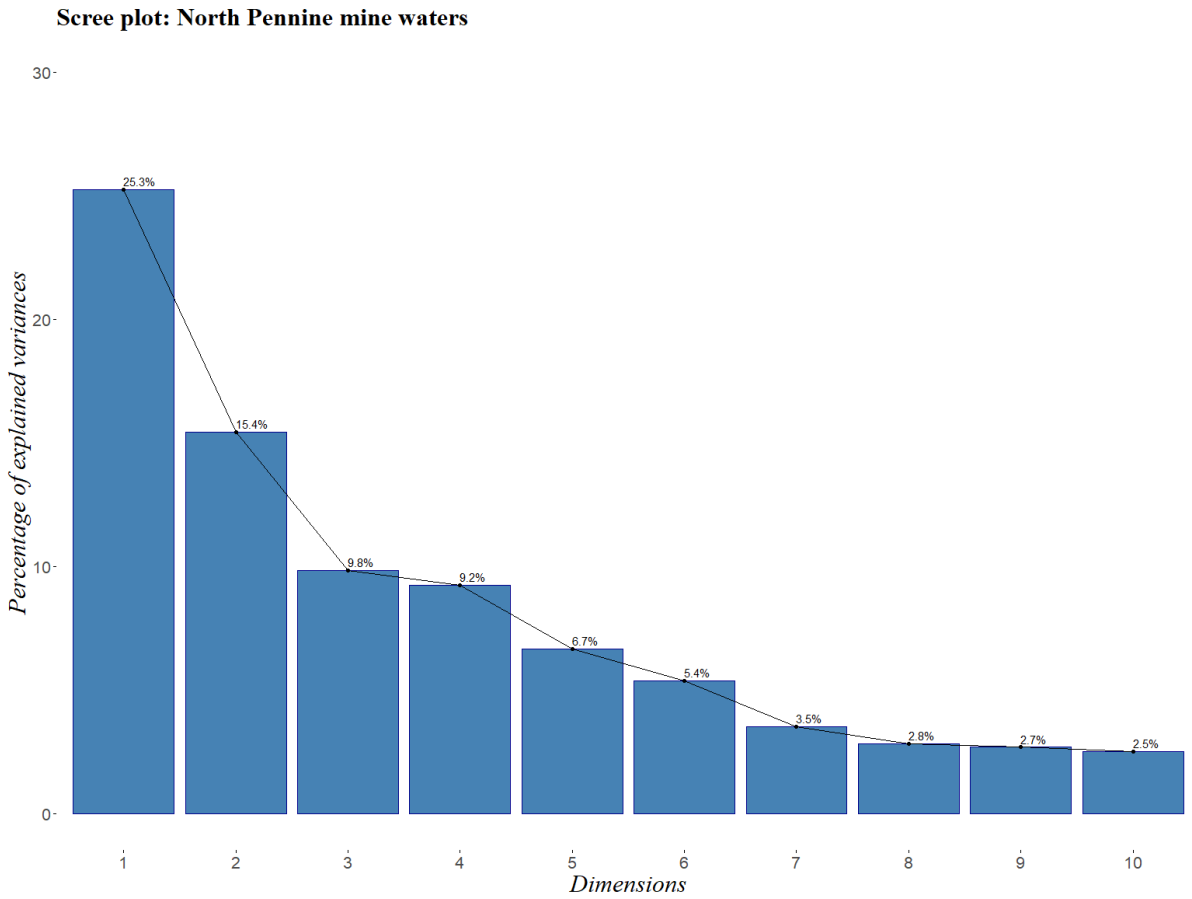


**Figure 4** Scree plot of principal component analysis of mine water samples, showing the variance explained by each principal component.

Pearson correlation coefficient (PCC) covariate analysis of the mine water chemistry identified similar variable relationships as the PCA (*Figure 5*). Li was found to have a positive correlation with Mn, As, conductivity, alkalinity, Ni, Ca, Sr, and Na, with a weaker correlation to Cl, $SO_4^{2-}$, Zn, S, and Mg. A very weak negative correlation was found between Li and Fe, V, P, and Ba. Conductivity had a positive correlation with all variables except for pH and $NO_3^-$, with a slight negative correlation for the former, and neutral for the latter. Conductivity was most strongly related to Cl, Ca, and K.

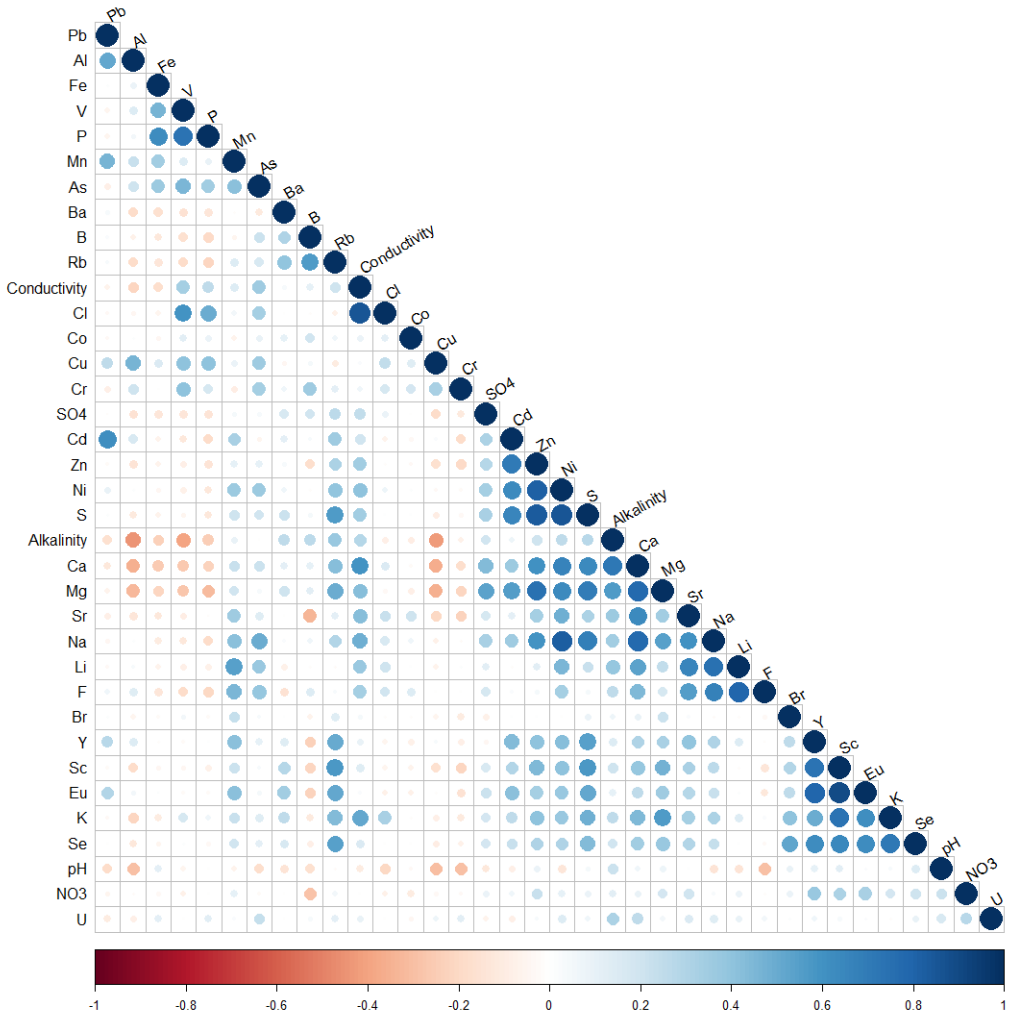


**Figure 5** Correlation matrix showing the Pearson correlation coefficient between variables in mine water samples.

ANOVA cluster analysis of the mine water variables identified Mg, F, Na, and conductivity as predictor analytes for Li (Figure 6). Similarly, conductivity, Na, and F were found related to Li by PCA, while the correlation coefficient matrix shows conductivity, Na, and Mg related to Li.

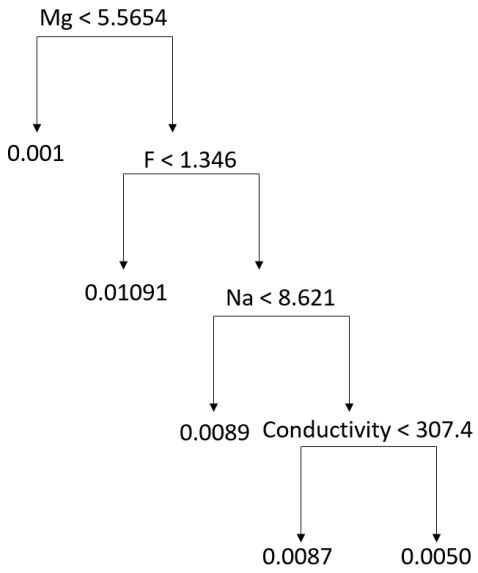


**Figure 6** Cluster analysis decision diagram of mine water samples. Cluster method = "ANOVA", outcome variable = "Li", predictor variables = all other variables.

Linear extrapolation connecting the two reference endmembers, in this case the 995 m Eastgate borehole sample and the "Capelcleugh high adit" mine water sample (*Figure 7a*) allows for the prediction of conservative mixing in the system. Most of the mine samples plot along this mixing line, with Cambokeels and the deep Scraithole sample serving as intermediary points between the more standard mine samples and the Eastgate borehole samples. A number of samples thought to be mine outflows that turned out to be drainage features unrelated to mine workings were removed from the plot, these include the two "hillside culvert" samples, which only flowed following heavy rain, a "high adit" sample near Nenthead which upon a return visit was discovered to be a drainage channel, and a "valley Debrah" sample, originally thought to be related to the Debrah mine.

The fit of this trend line justifies the use of Cl as a conservative element in mixing calculations, described earlier.

## 3.4 Conservative mixing for determining brine inputs to mine waters

The majority of mine samples plot along a Cl/Na mixing line ($R^2$ = 0.9959), with Cambokeels and the deep Scraithole sample serving as intermediary points between the mine samples with deeper brine inputs and the Eastgate borehole samples (*Figure 7*). Samples found to be drainage features unrelated to mine workings were removed, including the two "hillside culverts", which only flowed following heavy rain, a "high adit" sample near Nenthead which upon a return visit was discovered to be a drainage channel, and a "Valley Debrah" sample, originally thought to be related to the Debrah mine.

Despite being identified as a predictor variable for Li in the cluster analysis and correlation matrix, there was not a strong relationship between Mg and Li concentrations (Figure 7d), there appears to be three linear trends; the borehole samples, Cambokeels Mine samples, and the other mine outflows.

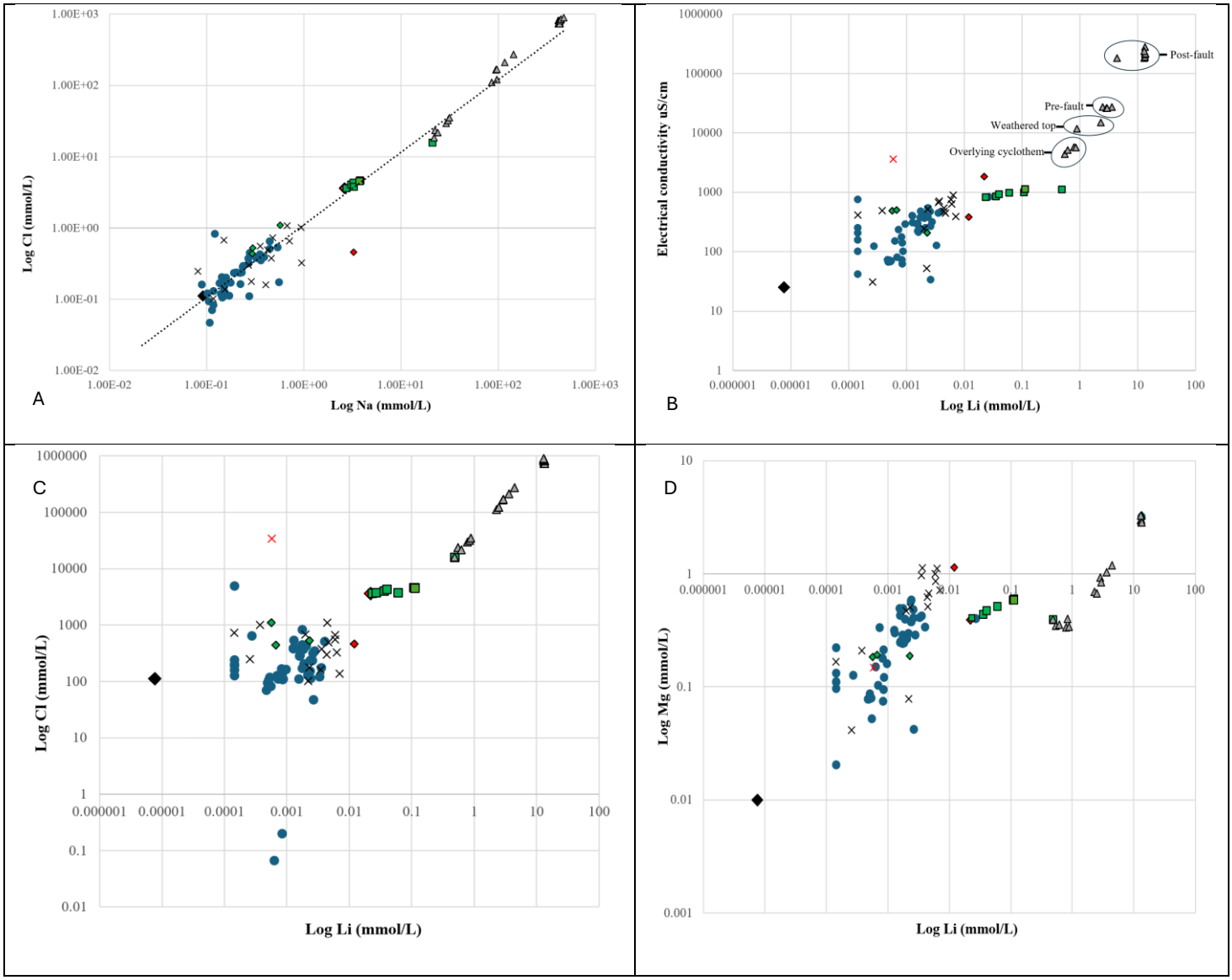


**Figure 7** Elemental ratios in sampled mine waters and the Eastgate Borehole (Manning *et al.* 2007): Top left (7a) Cl and Na (mmol/L) form a mixing line with $R^2$=0.9959. Top right (7b) Electrical conductivity (uS/cm) and Li (mmol/L). Bottom left (7c) Cl and Li (mmol/L). Bottom right (7d) Mg and Li (mmol/L). Symbology: Reference rainwater (Wilkinson et al. 1997) = Black diamond. Scraithole = Red diamonds. Eastgate borehole = Gray triangles. Cambokeels main outflow = Green squares. Cambokeels horse level = Green diamonds. Haggs, Barneycraig, and Coalcleugh mines = black X. All other mines = Blue dot. In figures 7b-7d the hillside culverts are denoted as a red x.

## 3.5 Prediction of elevated Li concentration in external data

Data from the Environment Agency (EA) WIMS database was ranked in order of variables which were linked to Li in the PCA and cluster analysis. Sites with potential elevated Li concentrations were predicted using ordering by conductivity and Na concentrations, however F was not included as a predictor due to a limited values in the WIMS database (480 of 850) and the lack of F measurements from the Eastgate borehole (*Figure 8*). The mines which ranked highly in both forms of ordering were: Scraithole mine, Barneycraig mine, Coalcleugh mine, Haggs Level at Nenthead, Ripsey Breakout Level, and Lord Carlisle Water Level. Each of these was below the

analytical detection limit in the WIMS database (100 µg/L), though the first four were sampled during our fieldwork

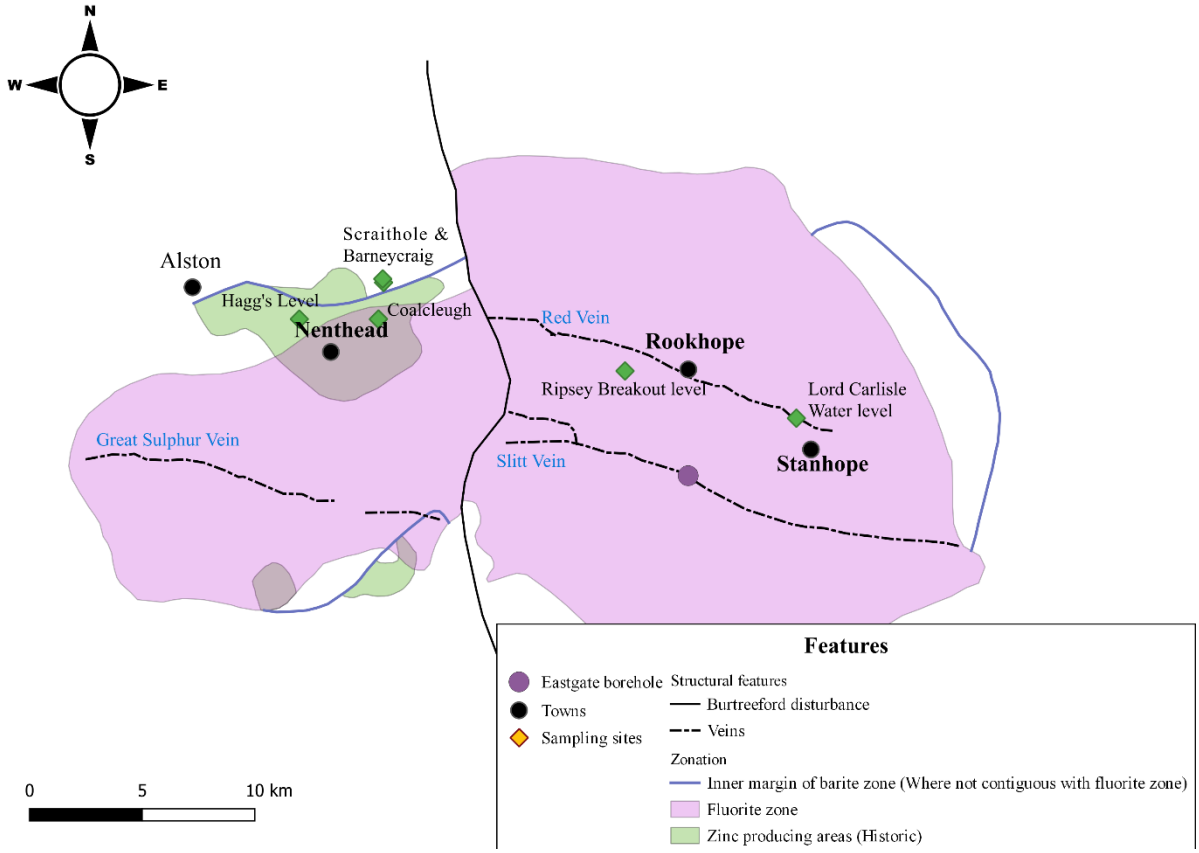


**Figure 8** A simplified map of the North Pennines which shows sampling locations which ranked highest for when ordered by the predictor variables identified by PCA and cluster analysis.

# 4. Discussion

Before this study, known Li resources in the region were solely connected to the Slitt Vein, specifically the Cambokeels mine and Eastgate borehole that intersected it. In analysing a wide range of mine outflows with methodology with a lower detection limit than the Environment Agency, the Scraithole mine (83 µg/L) and the Hagg's Level (49 µg/L) were mines with concentrations above the regional average (>24.2 µg/L). However, neither Scraithole nor the Hagg's Level are known to interact with the Slitt Vein. It could be that their Li outflows are unrelated to the deeper fluids, or multiple regional structural features are pathways by which the deeper fluids reach the near-surface.

A loading plot showing the contribution of each variable to principal components 1 and 2 (40.7% of total variance) in sampled mine waters (Figure 3) shows an association of Li with alkalinity, Ca, Cd, Cl, conductivity, F, K, Mg, Na, Se, and $SO_4^{2-}$; of these variables, Ca, Cl, conductivity, F, K, Mg, and Na are reported to increase with depth in the Eastgate Borehole (Manning et al. 2007). However, both alkalinity and dissolved $SO_4^{2-}$ are reported to decrease with depth. Further, there are no known Li minerals in the sedimentary cyclothems that overlie the Weardale Granite (Dunham 1990), or associated with the iron-, lead- and zinc-sulphides of the metal mineralisation (Ixer, Young, and Stanley 1996). The metal mineralisation is the most likely source of $SO_4^{2-}$ in

sampled mine waters. Despite this, there is a negative relationship between Li and Fe, and Pb, and a weak association of Li and Zn in the PCA output.

The only reported instances of Li >1 mg/L in groundwater were in the hydrothermal waters of the Eastgate Borehole (Manning et al. 2007) and the Cambokeels Mine (Manning and Strutt 1990), it is unlikely that the Li in the outflows of Scraithole and Hagg's Level differ in origin from that of Cambokeels outflow. The absence of other sources, and the common relationship between Li and F in micas (e.g. biotite, lepidolite, and zinnwaldite (Sanjuan et al. 2022)) found in granites, indicates the Weardale Granite is most probable source of Li in the geothermal brine of the North Pennines. Notably, the water chemistry reported by (Manning et al. 2007) showed little variation in Li concentrations from 410 to 996 m, 92.4 ± 1.6 mg/L whereas the host granite Li concentrations varied by 89.5 mg/kg over the same 724 m (271 m) (Figure 1). This is reflective of a well-mixed brine reservoir or more likely due to the failure of the packer used to seal the fracture at 410 m fully (Manning et al. 2007).

The movement of water up through the Weardale Granite has been proposed as the source of the metal mineralising hydrothermal fluids in the North Pennines (Colman, Ford, and Laffoley 1989; Sawkins 1966). Later models included alkali magma associated with the Whin Sill and Dyke Complex as additional heat sources driving convection in the Weardale Granite (Bott and Smith 2018). The mine workings sampled in this study result from this historic fluid movement, and the flow pathways of the mineralising fluid may still provide local connectivity from the underlying granite through overlaying sedimentary strata to the near-surface. The spring in the 100 m level of the Cambokeels mine, and elemental similarity to the brine samples from the Weardale Granite in the Eastgate borehole (Manning and Strutt 1990; Manning et al. 2007), provide evidence for potentially active flow pathways. If such linkages are present, upwelling modern fluids could be expected to have emanative centres and/or flow pathways along structural features similar to the mineralising fluid (Dempsey et al. 2021). Cambokeels Mine intersects the Slitt Vein near the centre of the Weardale Pluton. We hypothesised that mines near the Cambokeels and along the Slitt Vein would have significant contributions from deeper Li brine, and therefore have higher Li concentrations than the regional average. However, the mines central to the Weardale Pluton (White's Level, Governor & Co. Level, West Gate, Widley Level, an unnamed adit near to the Widley Level, and three springs including the Fairy Hole cave outflow in the Eastgate Quarry) were all below the average of 24.2 µg/L, with the highest of these being Widley Level (20.8 ± 9.4 µg/L). The Horse Level of Cambokeels mine has an average Li concentration of 54.2 µg/L, and is situated uphill from the main level, so the difference in Li concentration is likely a result of higher dilution from meteoric water, with the source of the Li in the outflow remaining the same. Cl and F values are consistent with this explanation, with the Cambokeels main level having averages of 132.91 mg/L and 3.56 mg/L, respectively, and the Horse Level 60.51 mg/L and 1.10 mg/L.

In contrast to our initial hypothesis, except for the Cambokeels Mine, the mine outflows with the highest Li concentrations were restricted to an area in the northwest of the North Pennines, around 8 km west of the furthest extent of the Slitt Vein (Dunham 1990). Additionally, these mines are not directly over plutons of the Weardale Granite. The mines are outside of the central fluorite zone and the proposed high-temperature emanative centres for mineralizing fluids (Dempsey et al. 2021). This indicates a decoupling of the modern brine system and the previous flow pathways for the highest-temperature mineralising fluids.

The majority of sampled mine waters differed chemically from both the borehole water and reference rainwater (Figure 7). The Eastgate Borehole water chemistry has relatively low alkalinity (55 mg/L as $CaCO_3$) and $SiO_2$ (9.6 mg/L) and contains significant Na and K (10,028 mg/L and 660

mg/L, respectively), and high Cl (27,692 mg/L), with trace elements such as Li, F, and B from dissolution of accessory minerals. Besides the low $SiO_2$ this chemistry is a typical granite-hosted geothermal water (Manning et al. 2007; Manning and Strutt 1990). Interpolation of Na/Cl mixing line from samples from the Eastgate Borehole and mine waters produces a mixing line with $R^2$ = 0.9959 (Fig 7a). The Cambokeels samples are between the borehole and other mine samples, which form a gradient along the mixing line towards reference rainwater (Wilkinson et al. 1997), likely a result of the higher contribution of deep brine to Cambokeels mine than the other mines.

Two-endmember mixing using these samples and Cl as the conservative species (summarised in Appendix Table 1) gives a relative contribution of geothermal fluids to Cambokeels mine outflow as 0.00577%. Samples taken from Scraithole Mine have a Li concentration of 83 µg/L at the outflow and 138 µg/L at 600 m into the mine, and the same mixing calculation gives a relative contribution from geothermal fluids of 0.00042% and 0.00137%, respectively. The average slope of the level of Scraithole mine that was sampled is <1%, but overburden increases rapidly because the mine is located on the side of a valley. The decrease reflects meteoric water infiltration near the mine portal.

To predict Li concentrations above the regional average of 24.2 µg/L in water samples from the WIMS database lacking Li measurements, samples were ordered by the elemental predictors based on PCA, PCC, and cluster analysis, conductivity, Mg, Na, Ni, and F. Summarised in Figure 8, the locations which were highlighted through this ordering were: Scraithole, Barneycraig, and Coalcleugh mines, Hagg's, Ripsey Breakout and Lord Carlisle Water levels. Of these, those sampled were Scraithole (83 - 138 µg/L), Barneycraig (2.6 - 41.2 µg/L), Coalcleugh (1.7 - 41.6 µg/L), and Hagg's Level (16.9 – 44.1 µg/L), all of which had samples above the regional average.

However, 57.5% sites in the WIMS data base lacked F measurements. In a second attempt using elements with lower predicted correlations but a higher level of occurrence in the data base was used; Na (95% representation), Cl (95.2%), Mg (97%), Sr (86.6%), and conductivity (96.6%). Through this method we can utilise existing databases which either have not measured the analyte of interest or for which the analyte of interest was below the detection limit of the method used.

## 4.2 Lithium in felsic systems

Although there is circumstantial evidence that the geologic source of the Li in the waters of the North Pennines is the Weardale Granite, there is no evidence for the mineral source of the Li in the granite. Globally, there are several types of Li-enrichments hosted in felsic systems, including geothermal brines, secondary clay deposits, ore-grade spodumene, and micas (Boschetti 2022; Millot, Négrel, and Petelet-Giraud 2007; Liu et al. 2020).

In the geothermal brines, the mineral source of Li varies but Li enrichment is commonly associated with micas and magmatic rocks rather than ore grade deposits due to the relative insolubility of spodumene. Less commonly, feldspars can contribute Li to geothermal brines, though this is often as a secondary source. Mica need not be associated with emplaced magmatic rocks such as granite and may be hosted in sedimentary strata such as sandstones (Sanjuan et al. 2016; Mroczek, Climo, and Evans 2015), though granites are a primary host.

Despite the close relationship between granites and mineral enrichment, the occurrence of Li brines hosted in granites is relatively rare and the exact conditions required for the Li enriched brine formation are unclear. Characteristics commonly associated with Li-enriched brines,

such as high TDS and Rb, are not always present in Li-enriched brines, and can be present in brines without Li (Bishop 2024).

Estimating the TDS of the Eastgate borehole using the electric conductivity and a conversion ratio of 0.75 for brines (Rusydi 2018), the Weardale Granite brine's TDS is 165,000 ppm. This falls between the URG (99,000 – 107,000 ppm TDS) and Cesano geothermal field (>300,000 ppm TDS). Our statistical analysis identifies conductivity as a potential predictor of elevated Li. Comparing conductivity converted to TDS and the reported Li concentrations of these fields shows that the highest Li concentration (480 mg/L) is reported in the Cesano field which has the highest TDS, though the lowest Li concentration is the Eastgate Borehole which does not have the lowest TDS. Likely, the relationship between TDS and Li extends only as far as hyper-saline brines commonly host higher Li concentrations, and any linearity between the two parameters is specific to each system.

Elevated Rb concentrations have been reported in the Li-enriched geothermal brines of Cornwall, Cesano, and URG (Sanjuan et al. 2016; Sanjuan et al. 2022; Dini et al. 2022). Rubidium was not measured in the waters of the Eastgate Borehole, and most of the mine water samples were below the detection limit for Rb (1.1 µg/L). Rubidium in the cuttings from the Eastgate Borehole varied from 34.8 to 86.5 mg/kg, lower than the average for felsic rocks (120 mg/kg) (USGS 2017). In granites, Rb commonly replaces K in K-feldspars, and mica (mainly biotite and muscovite). However, it is possible that in the hydrothermally altered sections of the Weardale Granite, Rb was lost during weathering, as evidenced by the higher Rb in the weathered clay-rich portions of the granite (81.95 ± 24.96 mg/kg at 275 m) compared to the average (56.68 ± 17.45 mg/kg), though the 915, 920, 950 and 995 m samples are also significantly higher than the average (61.25 ± 6.74 mg/kg, 74.92 ± 0.40 mg/kg, 86.40 ± 54.27 mg/kg, and 77.74 ± 0.95 mg/kg, respectively).

# 5. Conclusions

Statistical methods are an emerging tool that can play an important role in mineral exploration in areas where limited data exist. Relative to intrusive methods such as drilling boreholes, the statistical analysis of near surface waters in exploration is advantageous due to the minimal environmental impact, relatively low cost, and requirement of only a small number of sampling locations to produce acceptable results comparable with more geochemically involved studies.

Near-surface measurements need not be limited to mine workings. Springs, wells, shallow boreholes, and any area where there is potential for mixing with deeper fluids may be useful. The North Pennines act as a test for exploration like this; there is an unquantified but confirmed present resource, with prior indication of mixing. Through identification of proxy minerals and finding signals of the deeper geothermal system in a small number of mines not previously identified, a use case is demonstrated for near-surface measurements in the exploration of deeper resources.

- In the North Pennines, the Weardale Granite is the likely source of Li in the geothermal resource.

- The current subsurface fluid movement is likely decoupled from the hydrothermal system responsible for mineralisation of the North Pennines.

- In the mine waters of the North Pennines, PCA identified a relationship of Li with Alkalinity, Ca, Cd, Cl, F, K, Mg, Na, Se, and $SO_4^{2-}$ . Covariate analysis identified Li has a positive correlation with Mn, As, conductivity, alkalinity, Ni, Ca, Sr, and Na, with a weaker positive correlation to Cl, $SO_4^{2-}$, Zn, S, and Mg. Cluster analysis identified Mg, F, Na, and conductivity.

# 6. Acknowledgements

We thank Professor David Manning for providing cuttings from the Eastgate Borehole for destructive analysis. Also Dave Earley and Fiona Maclachlan for their technical support in the laboratory, Living Uplands for access to sites on their property, and the GeoNetZero CDT for funding and training support for this work. Finally, Leif, Tony and Nikita for their guidance and support in obtaining samples from within mines across the North Pennines, which would otherwise have been too dangerous.

# 7. References

Angino, Ernest E., and Gale K. Billings. 1966. 'Lithium content of sea water by atomic absorption spectrometry', *Geochimica et Cosmochimica Acta*, 30: 153-58.

Becker, R. A., Chambers, J. M. and Wilks, A. R. (1988) *The New S Language*. Wadsworth & Brooks/Cole.

Bishop, B.A., Robbins, L.J. 2024 (in review). Overview of basinal brine-hosted lithium mineral resources, distribution, and genesis in the Western Canada Sedimentary Basin. The Canadian Journal of Mineralogy and Petrology. Submission: CJMP-D-24-00035

Bishop, Brendan A., and Leslie J. Robbins. 2024. 'Using machine learning to identify indicators of rare earth element enrichment in sedimentary strata with applications for metal prospectivity', *Journal of Geochemical Exploration*, 258: 107388.

Boschetti, Tiziano. 2022. 'A revision of lithium minerals thermodynamics: Possible implications for fluids geochemistry and geothermometry', *Geothermics*, 98: 102286.

Bott, Martin H. P., and Frederick W. Smith. 2018. 'The role of the Devonian Weardale Granite in the emplacement of the North Pennine mineralization', *Proceedings of the Yorkshire Geological Society*, 62: 1-15.

Bowell, Robert J., Laura Lagos, Camilo R. de los Hoyos, and Julien Declercq. 2020. 'Classification and Characteristics of Natural Lithium Resources', *Elements*, 16: 259-64.

Carmona, V., J. J. Pueyo, C. Taberner, G. Chong, and M. Thirlwall. 2000. 'Solute inputs in the Salar de Atacama (N. Chile)', *Journal of Geochemical Exploration*, 69-70: 449-52.

Colman, T. B., T. D. Ford, and N. d'A Laffoley. 1989. 'Metallogeny of Pennine Orefields.' in J. A. Plant and D. G. Jones (eds.), *Metallogenic models and exploration criteria for buried carbonate-hosted ore deposits—a multidisciplinary study in eastern England: British Geological Survey The Institution of Mining and Metallurgy* (Springer US: Boston, MA).

Dempsey, E. D., R. E. Holdsworth, D. Selby, A. Bird, B. Young, and C. Le Cornu. 2021. 'A revised age, structural model and origin for the North Pennine Orefield in the Alston Block, northern England: intrusion (Whin Sill)-related base metal (Cu–Pb–Zn–F) mineralization', *Journal of the Geological Society*, 178: jgs2020-226.

Dini, Andrea, Pierfranco Lattanzi, Giovanni Ruggieri, and Eugenio Trumpy. 2022. 'Lithium Occurrence in Italy—An Overview', *Minerals*, 12: 945.

Dray, Stéphane, and Julie Josse. 2015. 'Principal component analysis with missing values: a comparative survey of methods', *Plant Ecology*, 216: 657-67.

Dunham, K. C. 1990. *Geology of the Northern Pennine Orefield*.

Dunham, K. C., G. A. L. Johnson, M. H. P. Bott, and B. L. Hodge. 1961. 'Granite beneath the Northern Pennines', *Nature*, 190: 899-900.

Ettehadi, Ali, Maksym Chuprin, Mehdi Mokhtari, Daniel Gang, Philip Wortman, and Ezat Heydari. 2024. 'Geological Insights into Exploration and Extraction of Lithium from Oilfield Produced-Water in the USA: A Review', *Energy & Fuels*.

Eymold, William K., Kelley Swana, Myles T. Moore, Colin J. Whyte, Jennifer S. Harkness, Siep Talma, Ricky Murray, Joachim B. Moortgat, Jodie Miller, Avner Vengosh, and Thomas H. Darrah. 2018. 'Hydrocarbon-Rich Groundwater above Shale-Gas Formations: A Karoo Basin Case Study', *Groundwater*, 56: 204-24.

Goldberg, Valentin, Ali Dashti, Robert Egert, Binil Benny, Thomas Kohl, and Fabian Nitschke. 2023. 'Challenges and Opportunities for Lithium Extraction from Geothermal Systems in Germany—Part 3: The Return of the Extraction Brine', *Energies*, 16: 5899.

Gruber, Paul W., Pablo A. Medina, Gregory A. Keoleian, Stephen E. Kesler, Mark P. Everson, and Timothy J. Wallington. 2011. 'Global Lithium Availability', *Journal of Industrial Ecology*, 15: 760-75.

H. Wickham (2016). Ggplot2: Elegant Graphics for Data Analysis. Springer-verlag, New York.

Han, Sun, Meng Zhenghao, Li Meilin, Yang Xiaohui, and Wang Xiaoxue. 2023. 'Global supply sustainability assessment of critical metals for clean energy technology', *Resources Policy*, 85: 103994.

Harkness, Jennifer S., Thomas H. Darrah, Nathaniel R. Warner, Colin J. Whyte, Myles T. Moore, Romain Millot, Wolfram Kloppmann, Robert B. Jackson, and Avner Vengosh. 2017. 'The geochemistry of naturally occurring methane and saline groundwater in an area of unconventional shale gas development', *Geochimica et Cosmochimica Acta*, 208: 302-34.

Jancsek, Krisztián, Patrick Janovszky, Gábor Galbács, and Tivadar M. Tóth. 2023. 'Granite alteration as the origin of high lithium content of groundwater in southeast Hungary', *Applied Geochemistry*, 149: 105570.

Kamienski, Conrad W., Daniel P. McDonald, Marshall W. Stark, and John R. Papcun. 2004. 'Lithium and Lithium Compounds.' in, *Kirk-Othmer Encyclopedia of Chemical Technology*.

Karaca, Z, DŞ Yücel, MA Yücel, and ZS Çetiner. 2013. 'Geothermal Sources and determination of their properties', *Geological Information System*.

Kassambara A, Mundt F (2020). _factoextra: Extract and Visualize the Result of Multivariate Data Analyses_. R package version 1.0.7, URL: https://cran.R-project.org/package=factoextra

Kavanagh, Laurence, Jerome Keohane, Guiomar Garcia Cabellos, Andrew Lloyd, and John Cleary. 2018. 'Global Lithium Sources—Industrial Use and Future in the Electric Vehicle Industry: A Review', *Resources*, 7: 57.

Kinch, Diana, and Jacqueline Holman. 2020. "New lithium supply chains could slash sector emissions by nearly a third: Roskill." In, edited by Richard Rubin. S&P Global: S&P Global.

Li, Chuan, Zilong Li, Tao Wu, Yaqin Luo, Jun Zhao, Xinren Li, Wencai Yang, and Xuegang Chen. 2021. 'Metallogenic characteristics and formation mechanism of Naomugeng clay-type lithium deposit in central inner Mongolia, China', *Minerals*, 11: 238.

Li, Jiexiang, Xinyi Wang, Chuanxia Ruan, Gideon Sagoe, and Jianlin Li. 2022. 'Enrichment mechanisms of lithium for the geothermal springs in the southern Tibet, China', *Journal of Hydrology*, 612: 128022.

Lindagato, Philemon, Yongjun Li, Jan Macháček, Gaoxue Yang, Irénée Mungwarakarama, Anastase Ndahimana, and Henri Patrick Kanimba Ntwali. 2023. 'Lithium Metal: The Key to Green Transportation', *Applied Sciences*, 13: 405.

Liu, Chen, Ru-Cheng Wang, Fu-Yuan Wu, Lei Xie, Xiao-Chi Liu, Xing-Kui Li, Lei Yang, and Xue-Jiao Li. 2020. 'Spodumene pegmatites from the Pusila pluton in the higher Himalaya, South Tibet: Lithium mineralization in a highly fractionated leucogranite batholith', *Lithos*, 358-359: 105421.

Manning, D. A. C., and D. W. Strutt. 1990. 'Metallogenetic significance of a North Pennine springwater', *Mineralogical Magazine*, 54: 629-36.

Manning, D. A. C., P. L. Younger, F. W. Smith, J. M. Jones, D. J. Dufton, and S. Diskin. 2007. 'A deep geothermal exploration well at Eastgate, Weardale, UK: a novel exploration concept for low-enthalpy resources', *Journal of the Geological Society*, 164: 371-82.

Mas-Fons, Aina, Rachel Horta Arudin, Philippe Loubet, Tina Pereira, Ashak Mahmud Parvez, and Guido Sonnemann. 2023. "Carbon and Water Footprints of Battery-Grade Lithium Carbonate Produced from Brine and Spodumene: A Study Focused on Process Simulation-Based Life Cycle Inventories." In.: Elsevier BV.

Miao, Y., L. Liu, K. Xu, and J. Li. 2023. 'High concentration from resources to market heightens risk for power lithium-ion battery supply chains globally', *Environ Sci Pollut Res Int*, 30: 65558-71.

Michael Friendly (2002). *Corrgrams: Exploratory displays for correlation matrices*. The American Statistician, 56, 316—324.

Millot, R., Ph Négrel, and E. Petelet-Giraud. 2007. 'Multi-isotopic (Li, B, Sr, Nd) approach for geothermal reservoir characterization in the Limagne Basin (Massif Central, France)', *Applied Geochemistry*, 22: 2307-25.

Mroczek, Edward Kazimierz, Melissa Climo, and David William Evans. 2015. *The composition of high temperature geothermal fluids in New Zealand producing geothermal fields* (GNS Science Taupo, New Zealand).

Munk, L.A., Hynek, S.A., Bradley, D.C., Boutt, D., Labay, K., and Jochens, H., 2016, Lithium Brines: A Global Perspective, in Rare Earth and Critical Elements in Ore Deposits: Society of Economic Geologists, p. 339–365.

Munk, Lee Ann, David F. Boutt, Scott A. Hynek, and Brendan J. Moran. 2018. 'Hydrogeochemical fluxes and processes contributing to the formation of lithium-enriched brines in a hyper-arid continental basin', *Chemical Geology*, 493: 37-57.

O'Sullivan, John, Naod Araya, Joris Popineau, Theo Renaud, Jeremy Riffault, and Mike O'Sullivan. 2024. 'Investigating Reinjection Strategies to Optimise Lithium Production from the Salton Sea Geothermal Field'.

Posit Team (2023). Rstudio: Integrated Development Environment for R. Posit Software, PBC, Boston, MA. URL: http://www.posit.co/

QGIS.org, 2023. QGIS Geographic Information System. QGIS Association. http://www.qgis.org

R Core Team (2023). R: A language and environment for statistical computing. R Foundation for statistical computing, Vienna, Austria. URL: https://www.R-project.org/

Rusydi, Anna F. 2018. 'Correlation between conductivity and total dissolved solid in various type of water: A review', *IOP Conference Series: Earth and Environmental Science*, 118: 012019.

Sanjuan, B., R. Millot, Ch Innocent, Ch Dezayes, J. Scheiber, and M. Brach. 2016. 'Major geochemical characteristics of geothermal brines from the Upper Rhine Graben granitic basement with constraints on temperature and circulation', *Chemical Geology*, 428: 27-47.

Sanjuan, Bernard, Blandine Gourcerol, Romain Millot, Detlev Rettenmaier, Elodie Jeandel, and Aurélien Rombaut. 2022. 'Lithium-rich geothermal brines in Europe: An up-date about

geochemical characteristics and implications for potential Li resources', *Geothermics*, 101: 102385.
Sawkins, FJ. 1966. 'Ore genesis in the North Pennine orefield, in the light of fluid inclusion studies', *Economic Geology*, 61: 385-401.
Stringfellow, William T., and Patrick F. Dobson. 2021. 'Technology for the Recovery of Lithium from Geothermal Brines', *Energies*, 14: 6805.
Suprapto, Sabtanto Joko, and Umi Yuliatin. 2020. 'POTENSI KANDUNGAN UNSUR KIMIA EKONOMIS PADA LARUTAN PANAS BUMI DENGAN STUDI KASUS DI PLTP DIENG, KABUPATEN WONOSOBO DAN KABUPATEN BANJARNEGARA, PROVINSI JAWA TENGAH', *Buletin Sumber Daya Geologi*, 15: 89-100.
Therneau T, Atkinson B (2022). _rpart: Recursive Partitioning and Regression Trees_. R package version 4.1.19, <https://CRAN.R-project.org/package=rpart>.

USGS. 2017. "Rubidium." In, edited by USGS.
———. 2021. 'Mineral Commodity Summaries: Lithium'.
———. 2022. 'Mineral Commodity Summaries: Lithium'.
———. 2023. 'Mineral Commodity Summaries: Lithium'.
———. 2024. "Mineral Commodity Summaries: Lithium." In
van den Boogaart, K. Gerald, and R. Tolosana-Delgado. 2008. '"compositions": A unified R package to analyze compositional data', *Computers & Geosciences*, 34: 320-38.
Vera, María L., Walter R. Torres, Claudia I. Galli, Alexandre Chagnes, and Victoria Flexer. 2023. 'Environmental impact of direct lithium extraction from brines', *Nature Reviews Earth & Environment*, 4: 149-65.
Vinante, D., and RN Alonso. 2006. 'Evapofacies of the Salar Hombre Muerto, Puna Argentina: distribution and genesis', *Magazine of the Argentine Geological Association*, 61: 286-97.
Vu VQ (2011). _ggbiplot: A ggplot2 based biplot. R package version 0.55, URL: http://github.com/vqv/ggbiplot

WANG, Chenguang, Mianping ZHENG, Xuefei ZHANG, Qian WU, Xifang LIU, Jianhong REN, and Shuangshuang CHEN. 2021. 'Geothermal-type Lithium Resources in Southern Xizang, China', *Acta Geologica Sinica - English Edition*, 95: 860-72.
Warren, John K. 2010. 'Evaporites through time: Tectonic, climatic and eustatic controls in marine and nonmarine deposits', *Earth-Science Reviews*, 98: 217-68.
Weinand, Jann Michael, Ganga Vandenberg, Stanley Risch, Johannes Behrens, Noah Pflugradt, Jochen Linßen, and Detlef Stolten. 2023. 'Low-carbon lithium extraction makes deep geothermal plants cost-competitive in future energy systems', *Advances in Applied Energy*, 11: 100148.
Wilkinson, J., B. Reynolds, C. Neal, S. Hill, M. Neal, and M. Harrow. 1997. 'Major, minor and trace element composition of cloudwater and rainwater at Plynlimon', *Hydrol. Earth Syst. Sci.*, 1: 557-69.

Yuan Tang, Masaaki Horikoshi, Wenxuan Li (2016). "ggfortify: Unfied Interface to Visualize Statistical Result of Popular R Packages." The R Journal 8.2, 2016: 478-489.

# 8. Appendix 1 (Extra figures)

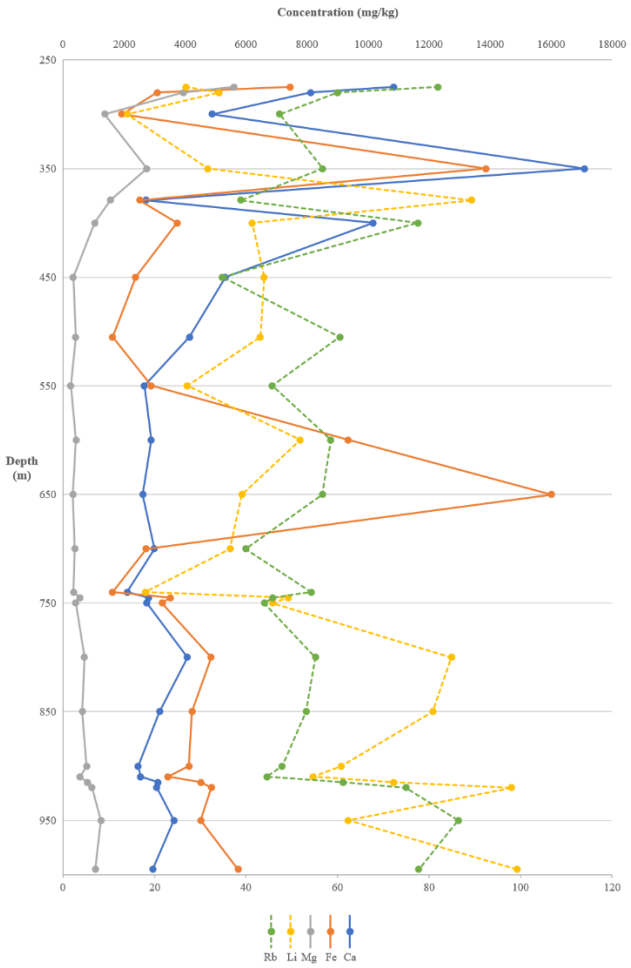


*Figure 9 Composite element depth profile of cutting from the Eastgate Borehole. Dashed lines are on the lower axis, solid lines are on the upper axis. Elements displayed determined by statistical analysis and understanding of the drill logs from* Manning et al. 2007.

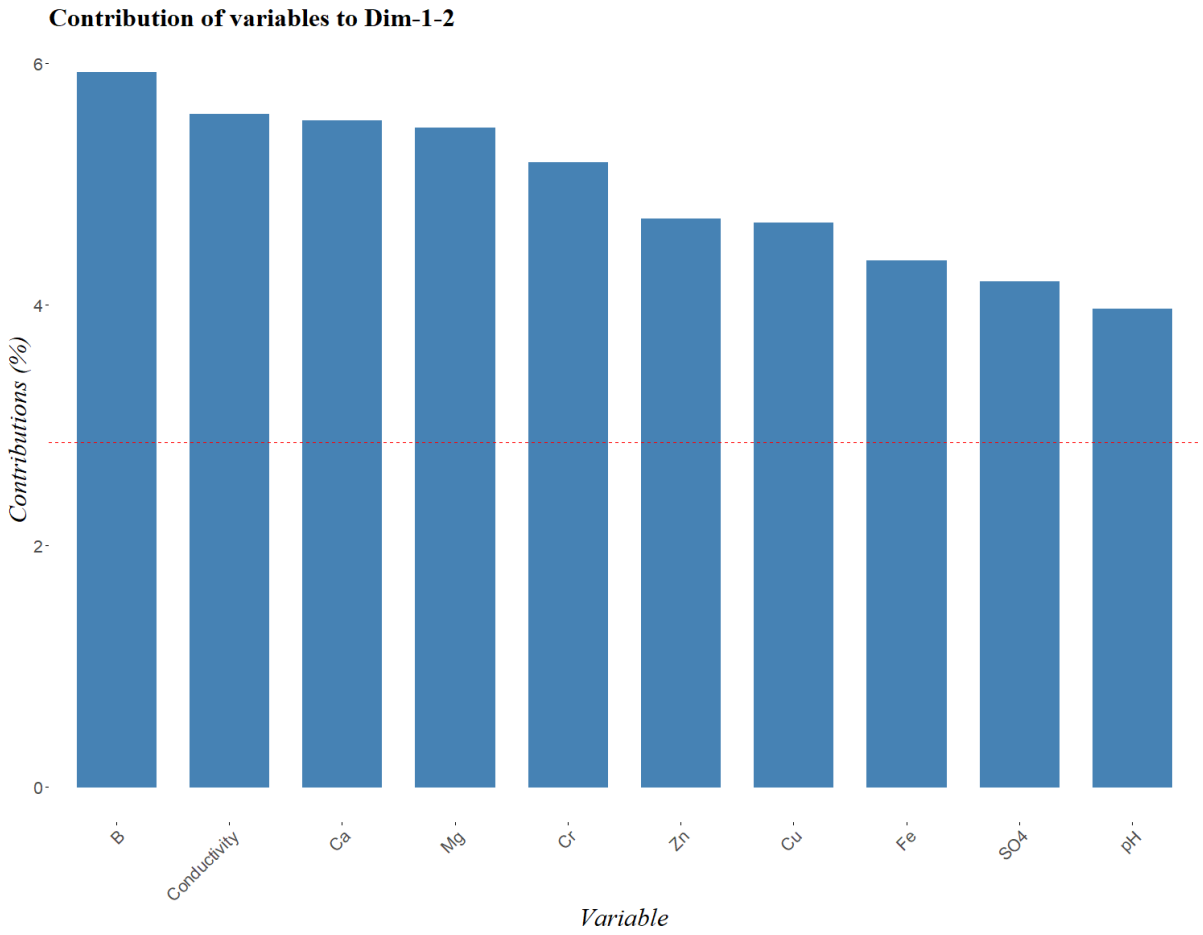


*Figure 10 Scree plot showing highest contributing variables to both PC1 and PC2 of mine water samples.*

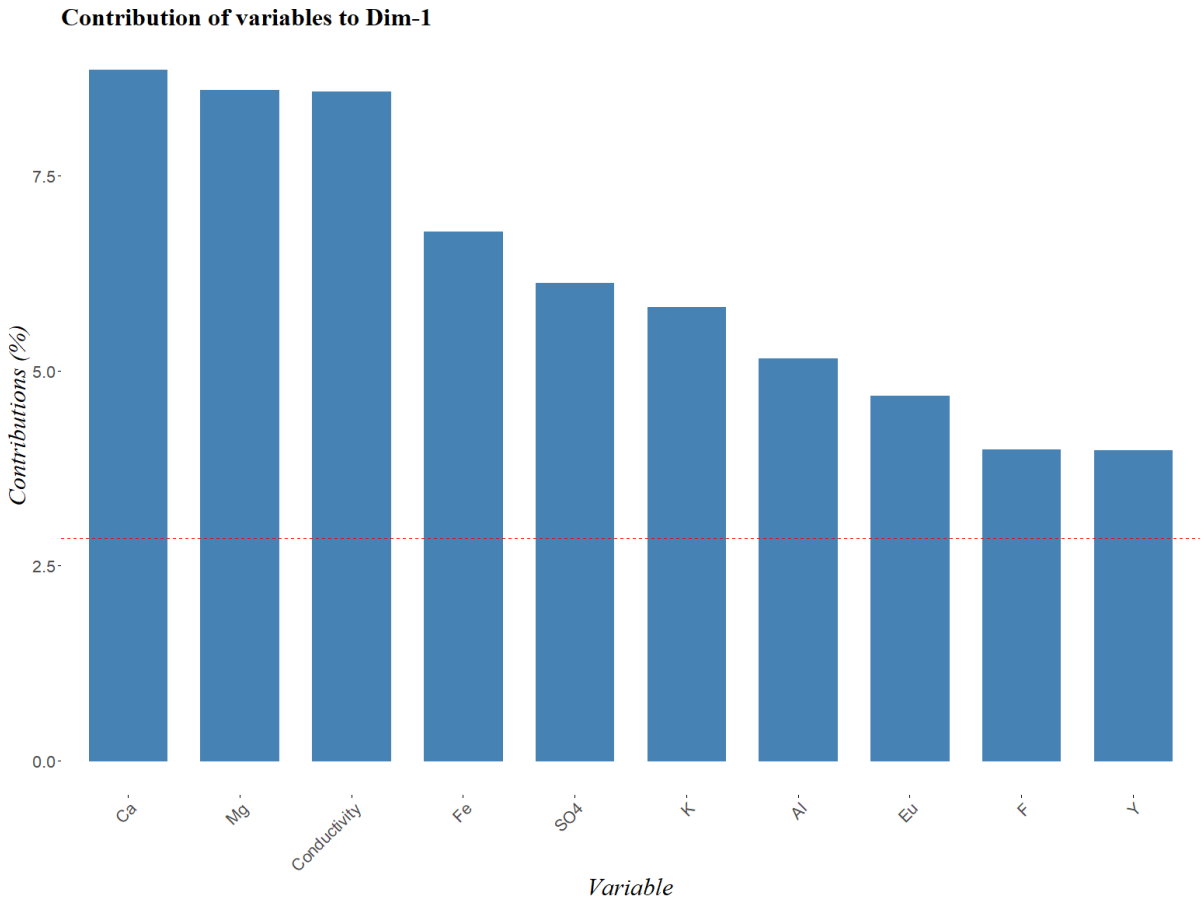


*Figure 11 Scree plot showing highest contributing variables to PC1 of mine water samples.*

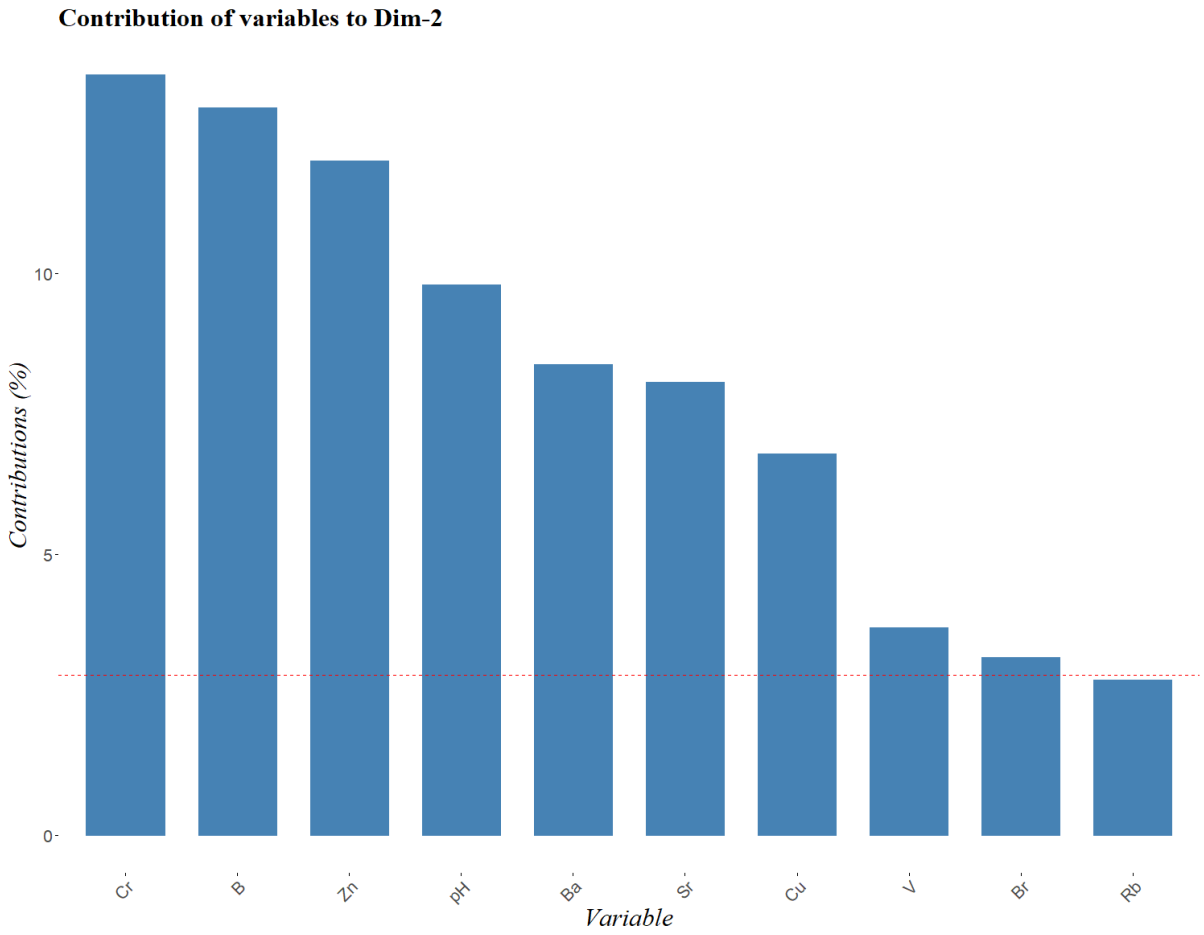


*Figure 12 Scree plot showing highest contributing variables to PC2 of mine water samples.*

*Table 1 Two endmember mixing calculation results using Cl as the conservative element and estimated source Li concentration.*

| Sample | Surface Contribution | Deep Contribution | Calculated Li concentration of source |
|---|---|---|---|
| Coalcleugh | 0.999841 | 0.000159 | 1123.346 |
| Deborah valley | 0.999319 | 0.000681 | 278.4263 |
| Barneycraig | 0.998875 | 0.001125 | 232.8253 |
| Cambokeels (horse) | 0.998779 | 0.001221 | 324.2918 |
| Hillside culvert | 0.957594 | 0.042406 | 9.572973 |
| Cambokeels (horse) | 0.999598 | 0.000402 | 1167.221 |
| New westernhope mine | 0.999992 | 8E-06 | 59891.21 |
| Eastgate Quarry sumping pool | 0.999938 | 6.2E-05 | 9170.796 |
| Ashcleugh mine | 0.999969 | 3.1E-05 | 18847.96 |
| Metal band 2 | 0.999944 | 5.6E-05 | 11862.5 |
| Rippon Level | 0.999664 | 0.000336 | 2592.733 |
| Rippon Level | 0.99965 | 0.00035 | 2513.702 |
| Hydrostream | 0.999471 | 0.000529 | 1683.35 |

| | | | |
|---|---|---|---|
| Capelcleugh | 0.999655 | 0.000345 | 3140.352 |
| Deborah | 0.999789 | 0.000211 | 5170.616 |
| Deborah lower | 0.99978 | 0.00022 | 5050 |
| Deborah lower | 0.999579 | 0.000421 | 2857.536 |
| Calvert | 0.999083 | 0.000917 | 1313.413 |
| Sir John's | 0.999937 | 6.3E-05 | 19269.84 |
| Deborah | 0.999675 | 0.000325 | 3894.14 |
| Whitesike level | 0.999892 | 0.000108 | 12083.33 |
| Smallcleugh | 0.999296 | 0.000704 | 1970.739 |
| Widley Level | 0.999606 | 0.000394 | 3592.085 |
| Whitesike adjacent mine | 0.999988 | 1.2E-05 | 123750 |
| Cambokeels | 0.999495 | 0.000505 | 3154.455 |
| Hagg's opposite river | 0.999931 | 6.9E-05 | 23318.84 |
| Bentyfield Mine Low level | 0.999959 | 4.1E-05 | 39731.71 |
| Governor and Co. Level | 0.999854 | 0.000146 | 11184.93 |
| Whites Level (Shaft) | 0.999853 | 0.000147 | 11217.69 |
| Whites Level | 0.999851 | 0.000149 | 11926.17 |
| Westernhope 2 | 0.999744 | 0.000256 | 7037.98 |
| Lord Carlisle water level | 0.999705 | 0.000295 | 6498.535 |
| High Capelcleugh | 1 | 0 | #DIV/0! |
| Capelcleugh | 0.999953 | 4.7E-05 | 52128.46 |
| Metal band 1 | 0.999931 | 6.9E-05 | 35594.2 |
| Rampgill | 0.999679 | 0.000321 | 7952.274 |
| Widley Level | 0.999493 | 0.000507 | 5417.954 |
| Smallcleugh | 0.999776 | 0.000224 | 13698.21 |
| Middlecleugh | 0.998783 | 0.001217 | 2550.534 |
| Middlecleugh | 0.999529 | 0.000471 | 6918.471 |
| Scaleburn | 0.999214 | 0.000786 | 4198.982 |
| Barneycraig | 0.999323 | 0.000677 | 6093.936 |
| Coalcleugh | 0.999452 | 0.000548 | 7594.781 |
| Hagg's Level | 0.999743 | 0.000257 | 17175.1 |
| Smallcleugh | 0.99998 | 2E-05 | 247228.9 |
| Scraithole | 0.99958 | 0.00042 | 19855 |
| Scraithole | 0.998629 | 0.001371 | 10088.84 |
| Cambokeels (horse) | 0.995557 | 0.004443 | 3466.126 |
| Cambokeels | 0.995532 | 0.004468 | 3655.998 |
| Cambokeels | 0.99541 | 0.00459 | 4068.845 |
| Cambokeels | 0.994996 | 0.005004 | 4960.546 |
| Cambokeels | 0.994654 | 0.005346 | 5215.612 |
| Cambokeels | 0.995356 | 0.004644 | 8986.597 |
| Cambokeels | 0.994291 | 0.005709 | 13075.25 |
| Cambokeels | 0.994226 | 0.005774 | 13591.34 |
| Cambokeels | 0.994399 | 0.005601 | 14013.94 |
| 135 | 0.980044 | 0.019956 | 17037.48 |
| 152 | 0.970438 | 0.029562 | 12854.34 |
| 166 | 0.972777 | 0.027223 | 15795.47 |

| | | | |
|---|---|---|---|
| 181 | 0.962847 | 0.037153 | 14803.65 |
| 192 | 0.959753 | 0.040247 | 14659.48 |
| 214.5 | 0.955867 | 0.044133 | 14048.44 |
| 234 | 0.860025 | 0.139975 | 11502.05 |
| 236.5 | 0.846822 | 0.153178 | 11359.33 |
| 266.5 | 0.732164 | 0.267836 | 9371.406 |
| 275 | 0.79113 | 0.20887 | 9623.211 |
| 300 | 0.787676 | 0.212324 | 9655.055 |
| 335 | 0.658879 | 0.341121 | 8999.739 |
| 411.5 | -0.03418 | 1.034178 | 8760.581 |
| 485 | 0.070515 | 0.929485 | 9865.678 |
| 561 | 0.029861 | 0.970139 | 9606.871 |
| 590 | 0.07699 | 0.92301 | 10075.73 |
| 674 | -0.02734 | 1.027342 | 9101.156 |
| 725 | 0.074472 | 0.925528 | 10026.71 |
| 770 | 0.075551 | 0.924449 | 10254.76 |
| 847 | -0.02159 | 1.021586 | 9230.745 |
| 910 | -0.07915 | 1.079149 | 8460.37 |
| 951 | -0.12232 | 1.122321 | 8134.928 |